

Influence of the Tool's Surface Microgeometry and the Lubricant Composition on Hole Precision in Hybrid Burnishing

N. Yu. Chikhacheva^{a,*}, A. V. Shchedrin^b, A. A. Bekaev^{b,**}, and T. A. Burlakova^{c,***}

^aAcademy of Quality Problems, Moscow, Russia

^bBauman Moscow State Technical University, Moscow, Russia

^cLikino-Dulyovo Preparatory School, Likino-Dulyovo, Russia

*e-mail: nadezhdachi@yandex.ru

**e-mail: bekaev@list.ru

***e-mail: ld-gim@yandex.ru

Received May 10, 2021; revised May 31, 2021; accepted June 10, 2021

Abstract—In the hybrid burnishing of holes in LS59-1 brass billets, for which grinding is not applicable, experiments are conducted to assess the dependence of the accuracy on the microgeometry of the tool's working surfaces and the composition of the lubricant ensuring wear-free operation of Garkunov–Kragelskii type.

Keywords: hybrid burnishing, hole, regular microrelief, wear-free condition, friction, machining accuracy

DOI: 10.3103/S1068798X2208010X

Statistical data indicate that hybrid burnishing, which combines deformation and cutting, is an effective means of producing high-quality holes in nonferrous copper–aluminum workpieces, for which grinding is not applicable [1, 2]. Depending on the hole depth, this method employs broaching or punching.

Today, improvement of hybrid burnishing is underway by combining regular microgeometry of the tool's working surfaces and an innovative metal-surfacing lubricant, which ensures wear-free operation of Garkunov–Kragelskii type [3–8].

In the present work, we investigate the influence of the tool's surface microgeometry and the composition of the metal-surfacing lubricant on the accuracy in hybrid burnishing of holes in nonferrous workpieces, for which grinding is not applicable.

The experimental workpieces are cylindrical LS 59-1 brass bushes (hardness 155 HB; external diameter 39 mm; length 40 mm). Before burnishing, the holes are reamed out to precision 0.03 mm, with surface roughness $Ra < 2.5 \mu\text{m}$.

The tool employed is a composite mandrel and broach, with P6M5 high-speed steel deforming elements.

The diameter of the deforming elements (over the calibration band) is 20.11–20.24 mm; the vertex angles of the working and inverse cones are 5° ; and the width of the calibration band is 7 mm.

Regular microrelief of the deforming surfaces (the working cone and calibration band) is created from the irregular microrelief obtained after grinding and polishing: single-pass helical channels (radius 1.5 mm, depth $D_{\text{ch}} = 8$ and $20 \mu\text{m}$) with spacing $S_{\text{ch}} = 0.5$ mm over the calibration band [5, 6].

In Fig. 1, we show longitudinal profilograms of the calibration bands. For the regular microrelief, the parameters $D_{\text{ch}} = S_{\text{ch}} = 0$ correspond to the initial irregular microrelief. The actual absolute deformation i_{ac} of the hole diameter in the workplace is 0.1–0.4 mm.

Burnishing at 0.05 m/min is undertaken using an R5 test machine. The baseline lubricant is I40 mineral oil, with Valena SV multifunctional metal-surfacing additive (Russian patent 2277579), which ensures wear-free operation of Garkunov–Kragelskii type [8].

The additive concentration is $C = 0, 10,$ and 20% .

After statistical analysis of the experimental data, we obtain the following expressions for the specific (linear) burnishing force (N/mm) [6, 7]:

• when $D_{\text{ch}} = S_{\text{ch}} = 0$

$$\left. \begin{aligned} q_b(C = 0) &= 89.86 + 506.67i_{\text{ac}}; \\ q_b(C = 10\%) &= 10.649 + 589.72i_{\text{ac}}; \\ q_b(C = 20\%) &= 13.76 + 565.41i_{\text{ac}}; \end{aligned} \right\} \quad (1)$$

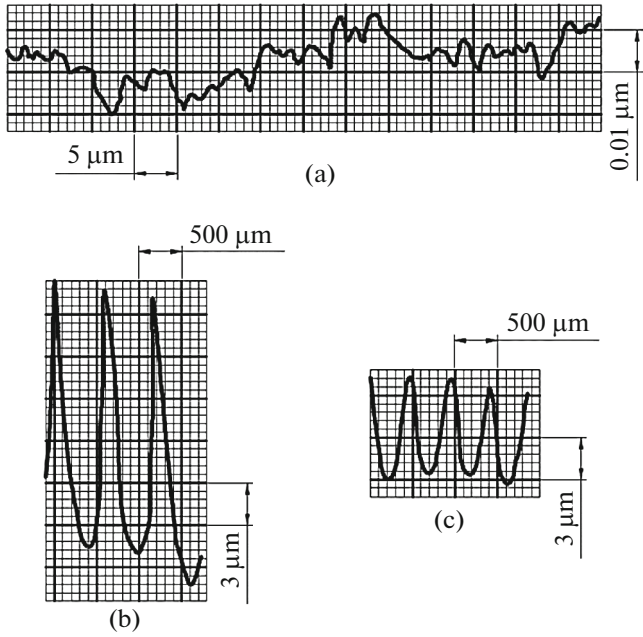


Fig. 1. Longitudinal profilograms of the calibration bands of deforming elements: (a) $D_{ch} = S_{ch} = 0$; (b) $D_{ch} = 20 \mu\text{m}$, $S_{ch} = 0.5 \text{ mm}$; (c) $D_{ch} = 8 \mu\text{m}$; $S_{ch} = 0.5 \text{ mm}$.

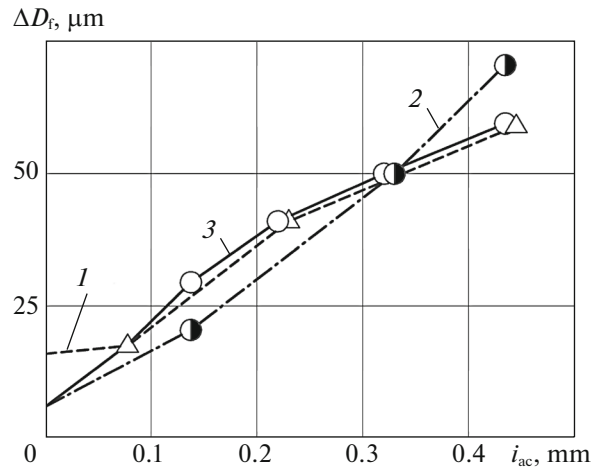


Fig. 2. Dependence of the scattering field ΔD_f of the final hole diameter on the actual absolute deformation i_{ac} when $D_{ch} = S_{ch} = 0$ and the additive concentration $C = 0$ (1), 10% (2), and 20% (3).

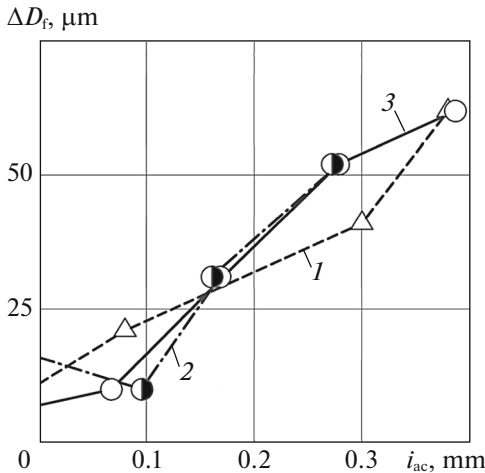


Fig. 3. Dependence of the scattering field ΔD_f of the final hole diameter on the actual absolute deformation i_{ac} when $D_{ch} = 8 \mu\text{m}$, $S_{ch} = 0.5 \text{ mm}$, and the additive concentration $C = 0$ (1), 10 (2), and 20% (3).

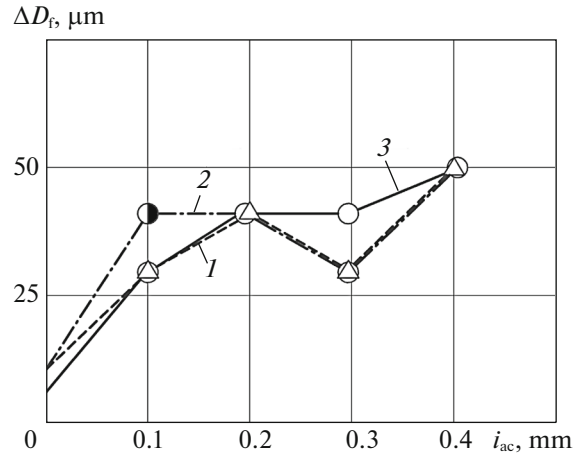


Fig. 4. Dependence of the scattering field ΔD_f of the final hole diameter on the actual absolute deformation i_{ac} when $D_{ch} = 20 \mu\text{m}$, $S_{ch} = 0.5 \text{ mm}$, and the additive concentration $C = 0$ (1), 10 (2), and 20% (3).

- when $D_{ch} = 8 \mu\text{m}$ and $S_{ch} = 0.5 \text{ mm}$

$$\left. \begin{aligned} q_b(C = 0) &= 176.97 + 569.53i_{ac}; \\ q_b(C = 10\%) &= 162.56 + 341.54i_{ac}; \\ q_b(C = 20\%) &= 66.05 + 802.1i_{ac}; \end{aligned} \right\} \quad (2)$$
- when $D_{ch} = 20 \mu\text{m}$ and $S_{ch} = 0.5 \text{ mm}$

$$\left. \begin{aligned} q_b(C = 0) &= 149.45 + 980.11i_{ac}; \\ q_b(C = 10\%) &= 102.93 + 1160.39i_{ac}; \\ q_b(C = 20\%) &= 164.65 + 894.64i_{ac}. \end{aligned} \right\} \quad (3)$$

Analysis of Eqs. (1) and (2) shows that the additive may decrease the unit broaching force by 18–23.8%. This is explained as follows: a protective film whose

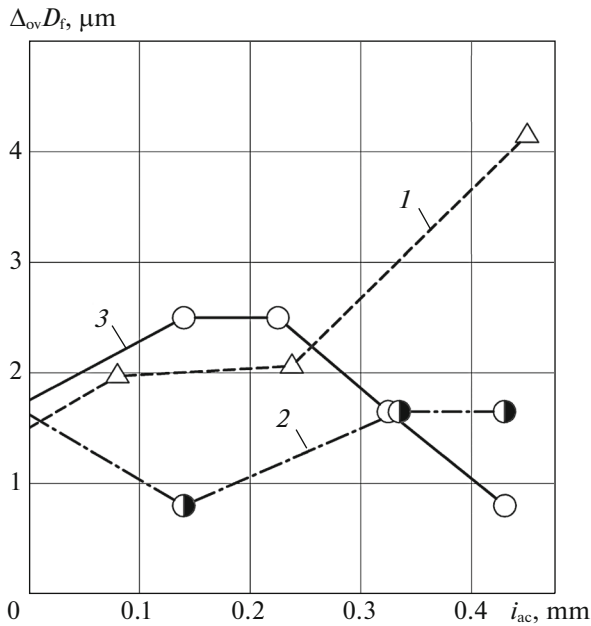


Fig. 5. Dependence of the oval distortion $\Delta_{ov}D_f$ of the final hole on the actual absolute deformation i_{ac} when $D_{ch} = S_{ch} = 0$ and the additive concentration $C = 0$ (1), 10 (2), and 20% (3).

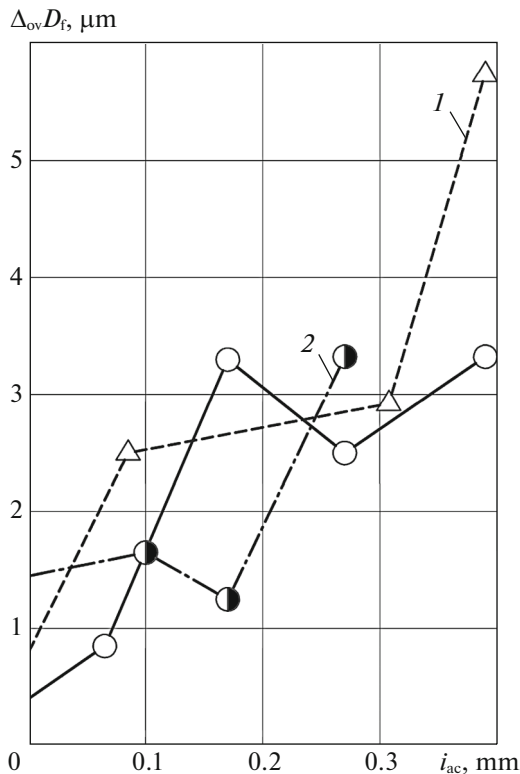


Fig. 6. Dependence of the oval distortion $\Delta_{ov}D_f$ of the final hole on the actual absolute deformation i_{ac} when $D_{ch} = 8 \mu m$, $S_{ch} = 0.5 mm$, and the additive concentration $C = 0$ (1), 10 (2), and 20% (3).

properties prevent direct contact of the rough tool and workpiece surfaces is formed in the deformation zone; the Rehbinder effect is intensified; and the adhesive component of the slipping friction coefficient is significantly decreased [8, 9]. In addition, with no change in the unit broaching force, the lubricant containing Valena SV additive permits doubling of the deformation i_{ac} on account of plasticization of the hole's surface layer. That increases the productivity in hole shaping.

As we see in Fig. 1 and Eqs. (2) and (3), there is no change in the force when broaching by a tool with regular microrelief for which $D_{ch} = 20 \mu m$ and $S_{ch} = 0.5 mm$. That may be explained by the parallel action on the workpiece in microcutting, as indicated by the microchip densely packed in the channels of the regular microrelief for all types of lubricant [4, 9]. The microcutting is due to the small longitudinal radius (6–12 μm) at the tips of the microprojections when $D_{ch} = 20 \mu m$ and $S_{ch} = 0.5 mm$ [5, 6]. As a result, the metal-surfacing lubricant does not accumulate in the channels of the regular microrelief and does not minimize the friction.

In Figs. 2–4, we show the general scattering pattern for the hole diameter in the final sample. On that basis, the dimensional accuracy may be assessed.

To plot Figs. 2–4, the hole in each final sample is measured by means of inside calipers in four diagonal

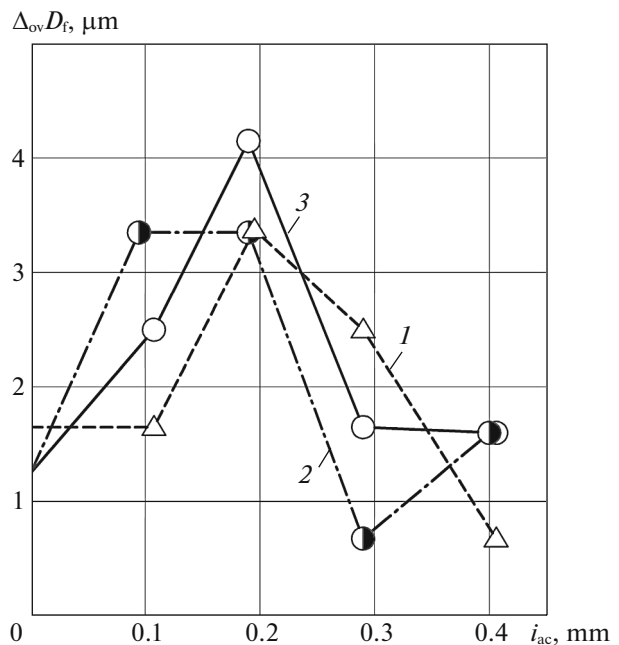


Fig. 7. Dependence of the oval distortion $\Delta_{ov}D_f$ of the final hole on the actual absolute deformation i_{ac} when $D_{ch} = 20 \mu m$, $S_{ch} = 0.5 mm$, and the additive concentration $C = 0$ (1), 10 (2), and 20% (3).

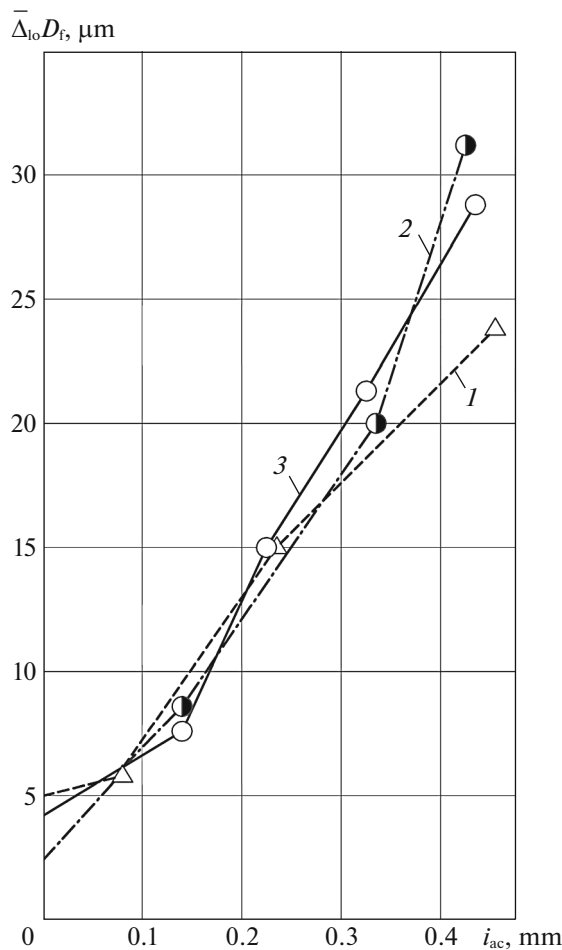


Fig. 8. Dependence of the mean longitudinal deviation $\bar{\Delta}_{10}D_f$ of the final hole on the actual absolute deformation i_{ac} when $D_{ch} = S_{ch} = 0$ and the additive concentration $C = 0$ (1), 10 (2), and 20% (3).

cross sections and three vertical cross sections, as for the holes in the workpieces [10].

Analysis of Figs. 2–4 shows that, by ensuring regular microrelief of the tool surfaces and employing metal-surfacing lubricants, the dimensional prediction of the final holes may be improved even with relatively precise dimensions of the workpiece holes (curve 2, Fig. 3) [10, 11].

The higher quality (smaller dimensional error ΔD_f) when using a tool with regular microrelief for which $D_{ch} = 20 \mu\text{m}$ and $S_{ch} = 0.5 \text{ mm}$ may be attributed to the parallel microcutting [10, 11].

To better understand the formation of dimensional precision (Figs. 2–4), we plot the mean oval distortion (Figs. 5–7) and the deviation of the longitudinal profile (Figs. 8–10) of the holes in the final samples by the same method [10, 12, 13]. Their analysis shows that the dimensional precision (Figs. 2–4) depends mainly on the deviation of the longitudinal hole pro-

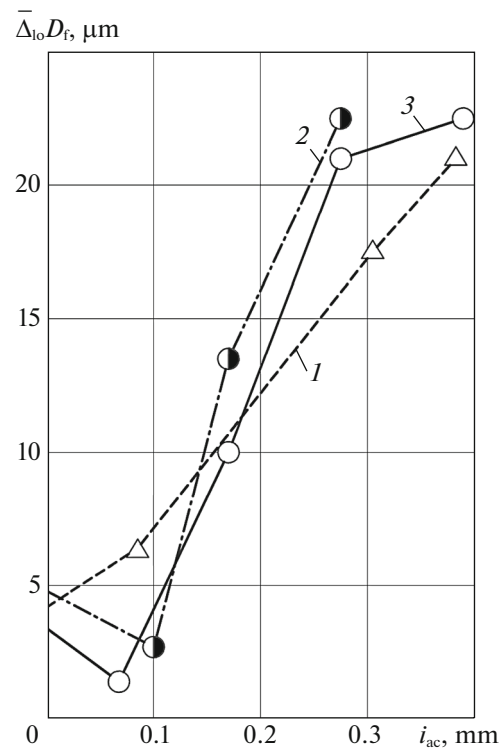


Fig. 9. Dependence of the mean longitudinal deviation $\bar{\Delta}_{10}D_f$ of the final hole on the actual absolute deformation i_{ac} when $D_{ch} = 8 \mu\text{m}$, $S_{ch} = 0.5 \text{ mm}$, and the additive concentration $C = 0$ (1), 10 (2), and 20% (3).

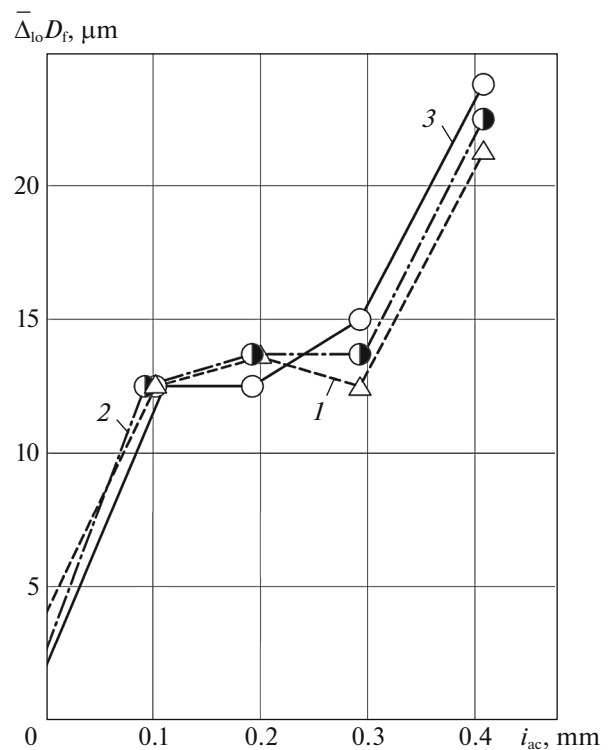


Fig. 10. Dependence of the mean longitudinal deviation $\bar{\Delta}_{10}D_f$ of the final hole on the actual absolute deformation i_{ac} when $D_{ch} = 20 \mu\text{m}$, $S_{ch} = 0.5 \text{ mm}$, and the additive concentration $C = 0$ (1), 10 (2), and 20% (3).

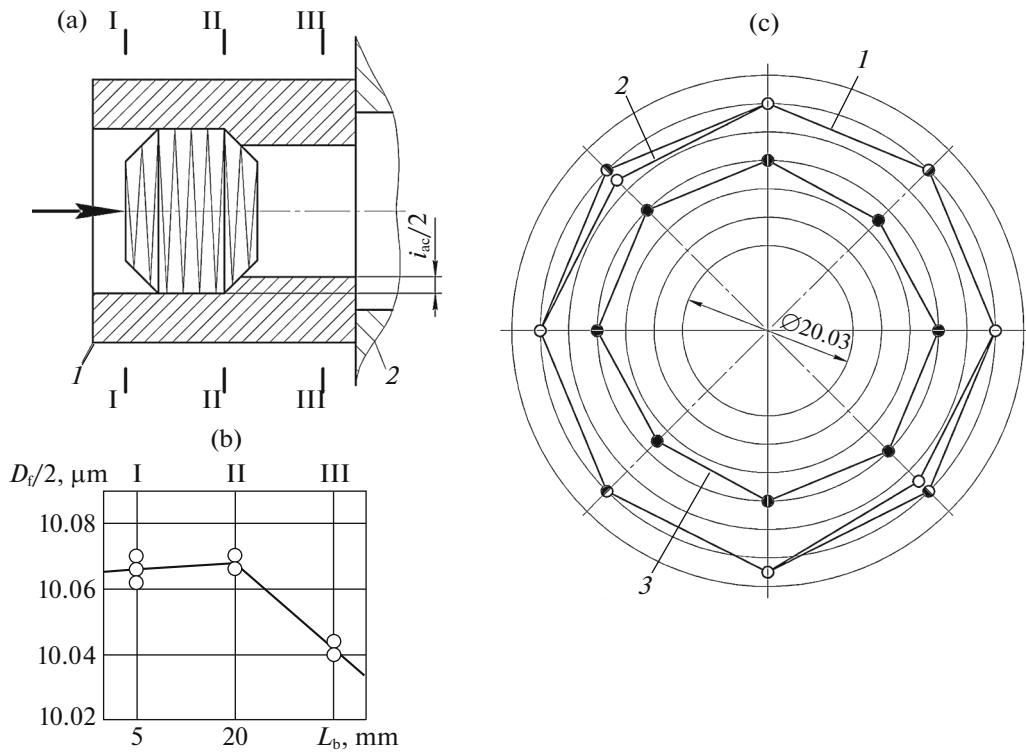


Fig. 11. Typical mean longitudinal profile of the final hole (a), burnishing configuration (b), and typical polar diagrams of the final holes (c) in vertical cross sections I–I (1), II–II (2), III–III (3) after burnishing when $i_{ac} = 0.387$ mm, $C = 20\%$; $D_{ch} = 8$ μm , and $S_{ch} = 0.5$ mm.

file (Figs. 8–10), for which the geometric error is greater than for the oval distortion (Figs. 5–7)

$$\Delta D_f \approx 2(\Delta_{ov} D_f + \Delta_{lo} D_f),$$

where D_f is the diameter of the final hole in cross sections I–III, mm.

The total increase in mean longitudinal deviation of the final hole with increase in the actual absolute deformation i_{ac} (Figs. 8–10) is a consequence of the nonuniform radial rigidity of the workpieces over the height. The radial rigidity is less at the upper (input) end (Fig. 11a, cross section I–I) of workpiece 1 than at the lower (output) end (Fig. 11a, cross section III–III), on account of the reactive frictional forces at the surface of broaching attachment 2 in machining.

The reactive frictional forces are directly proportional to the broaching forces, as is evident from Eqs. (1)–(3).

In studying the formation of the geometric accuracy, we plot both the mean longitudinal profiles of the final holes (Fig. 11a) and polar diagrams (Fig. 11c) in the corresponding vertical cross sections I–III.

Analysis of curves 1 and 2 in Fig. 11c shows that there is little difference in the oval distortion of the final holes in cross sections I and II (Fig. 11a).

The smaller area of curve 3 in vertical cross section III (Fig. 11c) is associated with the reactive fric-

tional forces at the supporting (output) end of the workpieces (Fig. 11a), where the hole radius and diameter are least in the final samples.

Thus, by varying the microgeometry of the tool's working surfaces and the lubricant composition (on the basis of the physical principles in [8]), we may control the accuracy of holes produced by hybrid burnishing [9–13]. On the basis of the results, the information base for artificial intelligence algorithms may be expanded, while the fundamental principles of tribology based on self-organization [3–5, 8] may be adapted to the synthesis of new hybrid burnishing methods [14, 15].

REFERENCES

1. Rozenberg, A.M., Rozenberg, O.A., Posvyatenko, E.K., et al., *Raschet i proektirovanie tverdospilnykh deformiruyushchikh protyazhek i protsessa protyagivaniya* (Calculation and Design of Carbide Deforming Broaches and the Broaching Process), Kiev: Naukova Dumka, 1978.
2. Proskuryakov, Yu.G., Romanov, V.N., and Isaev, A.N., *Ob'emnnoe dornovanie otverstii* (Volumetric Mandrel of Holes), Moscow: Mashinostroenie, 1984.

3. Shchedrin, A.V., Kostryukov, A.A., and Chikhacheva, N.Yu., Artificial technological intelligence as the ideological basis of the generalized system of materials processing methods, *Uproch. Tekhnol. Pokryt.*, 2015, no. 6, pp. 20–26.
4. Shchedrin, A.V., Ignatkin, I.Yu., and Chikhacheva, N.Yu., Systemic formation of information databases of characteristics of processing methods for implementation of algorithmic procedures of artificial technological intelligence, *Uproch. Tekhnol. Pokryt.*, 2020, vol. 16, no. 10, pp. 444–451.
5. Shchedrin, A.V., Tanengol'ts, A.B., Egorova, Z.I., et al., Tribological concept of system analysis-synthesis of combined methods of deformation-cutting processing, *Tekh. Mashinostr.*, 2001, no. 4 (32), pp. 53–59.
6. Shchedrin, A.V., Ignatkin, I.Yu., Bugaev, A.M., et al., Study of power dynamics characteristics of combined mandrelling methods of holes by regular surface microgeometry tool, *Uproch. Tekhnol. Pokryt.*, 2020, vol. 16, no. 8, pp. 360–365.
7. Shchedrin, A.V., Bekaev, A.A., Ignatkin, I.Yu., et al., Effect of composition of metal-cladding lubricant and its application technology on contact characteristics of combined hole mandrelling methods, *Uproch. Tekhnol. Pokryt.*, 2020, vol. 16, no. 11, pp. 504–510.
8. Garkunov, D.N., Mel'nikov, E.L., Babel', V.G., et al., *Tribologiya na osnove samoorganizatsii* (Tribology Based on Self-Organization), Saarbrücken: Lambert Academic, 2015.
9. Shchedrin, A.V., Ignatkin, I.Yu., and Chikhacheva, N.Yu., Study of variation patterns in sliding friction coefficient in innovative methods of combined hole mandrelling, *Uproch. Tekhnol. Pokryt.*, 2020, vol. 16, no. 4, pp. 150–155.
10. Shchedrin, A.V., Ulyanov, V.V., Bekaev, A.A., and Chikhacheva, N.Yu., Efficient hole broaching with regularized surface microgeometry of the deforming elements, *Russ. Eng. Res.*, 2009, vol. 29, no. 9, pp. 911–915.
11. Shchedrin, A.V., Aleshin, V.F., Mel'nikov, E.L., et al., Study of formation regularities of surface layer quality parameters during cutting on prestrained layer in methods of combined hole burnishing, *Remont, Vosstan., Modern.*, 2020, no. 1, pp. 23–28.
12. Sergeev, E.S., Zinin, M.A., Gavrilov, S.A., et al., Influence of the angle of deflection member surfaces affect the performance of the combined methods of suturing (drawing) of the holes, *Uproch. Tekhnol. Pokryt.*, 2015, no. 3, pp. 20–24.
13. Shchedrin, A.V., Aleshin, V.F., Bugaev, A.M., et al., Technological capabilities of combined mandrelling method of holes by acting surfaces helical geometry tools, *Uproch. Tekhnol. Pokryt.*, 2019, vol. 15, no. 8, pp. 342–347.
14. Vorontsov, A.L., Industrial testing of the results of a combined reduction-mandrelling process researching, *Kuznechno-Shtamp. Proizvod. Obrab. Mater. Davlen.*, 2017, no. 9, pp. 3–10.
15. Shchedrin, A.V., Aleshin, V.F., Bekaev, A.A., and Chikhacheva, N.Yu., Hybrid burnishing of cylindrical workpieces with a modified hole surface, *Russ. Eng. Res.*, 2020, vol. 40, no. 10, pp. 852–856.

Translated by B. Gilbert